Fuel 137 (2014) 339–345

Contents lists available at ScienceDirect

Fuel

journal homepage: www.elsevier.com/locate/fuel

Laminar flame speed and Markstein length of syngas at normal and elevated pressures and temperatures

Yuhua Ai [a], Zhen Zhou [a,b], Zheng Chen [c], Wenjun Kong [a,*]

[a] Key Laboratory of Light-duty Gas-turbine, Institute of Engineering Thermophysics, Chinese Academy of Sciences, Beijing 100190, China
[b] University of Chinese Academy of Sciences, Beijing, China
[c] SKLTCS, Department of Mechanics and Engineering Science, College of Engineering, Peking University, Beijing 100871, China

HIGHLIGHTS

- Measured laminar flame speeds and Markstein lengths of syngas.
- Compared experimental data with predictions from various kinetic models for syngas.
- Assessed the effects of Lewis number and flame temperature using various oxidizers.
- Examined the effects of pressure and initial temperature.

ARTICLE INFO

Article history:
Received 11 April 2014
Received in revised form 3 August 2014
Accepted 4 August 2014
Available online 20 August 2014

Keywords:
Syngas
Propagating spherical flame
Laminar flame speed
Markstein length
Lewis number

ABSTRACT

Synthetic gas, or syngas, is a popular alternative fuel for gas turbine industry. However, the composition of syngas is complex which complicates the combustor design. In this study, a dual-chambered pressure-release type combustion apparatus was developed and used for measurements of laminar flame speed which could be operated at high pressures and temperatures. The laminar flame speeds of syngas were measured at normal and elevated pressures and temperatures. The effects of Lewis number, flame temperature, pressure and initial temperature on the laminar flame speed and Markstein length of typical syngas mixtures were investigated. The results showed that the unstretched laminar flame speed increased with the increase of Lewis number and flame temperature, and that it decreased with the increase of pressure. The Markstein length decreased with the increase of pressure and initial temperature. It was found that the Markstein length was less sensitive to change of initial temperature than that of pressure. Furthermore, the performance on theoretical model for Markstein length using different Lewis numbers was examined. It was found that for syngas, the diffusion-based effective Lewis number rather than the volume or heat release-based Lewis number should be used to evaluate the Markstein length from the theoretical model.

1. Introduction

Currently, syngas (synthesis gas) is expected to play an important role in future energy production, particularly for stationary power generation using Integrated Gasification Combined Cycle (IGCC) systems. Syngas is essentially composed of CO, H_2, N_2, CO_2 and H_2O [1]. The syngas composition and proportions of every constituent can vary widely due to various types of chosen feedstock and various methods of gasification process. This brings a challenge for combustor designers since typical combustor design tools require data on various fundamental gas combustion properties in order to design an efficient fuel flexible combustor. Therefore, it is an essential topic to study the fundamental burning properties of syngas over a wide range of composition under representative operating conditions of advanced gas turbines. Recently, various investigations have been conducted [2–7].

Laminar flame speed and Markstein length are two most fundamental physicochemical properties of a combustible mixture. They can be used to validate and develop chemical kinetic mechanisms of different fuels. They are also important input parameters for modeling turbulent premixed combustion within the laminar flamelet regime [8]. In the literature, several studies have been conducted to measure the laminar flame speeds of syngas using outwardly propagating spherical flames. McLean and coworkers [9,10] measured the laminar flame speed of H_2/CO

* Corresponding author. Tel./fax: +86 10 8254 3042.
E-mail address: wjkong@iet.cn (W. Kong).

http://dx.doi.org/10.1016/j.fuel.2014.08.004
0016-2361/

mixtures consisting of 5–100% H_2 (in volume) at various equivalence ratios. Sun et al. [11] studied the laminar flame speed of H_2/CO/air and H_2/CO/O_2/He mixtures at high pressures up to 4 MPa. Burke et al. [12] measured the laminar flame speed of H_2/CO/O_2/diluent at low adiabatic flame temperature and high pressure (up to 2.5 MPa). Prathap et al. [13,14] investigated the effect of nitrogen and carbon dioxide dilution on laminar flame speed and Markstein length of syngas at atmospheric pressure. Kéromnès et al. [15] measured the laminar flame speed of H_2/CO/O_2/He mixtures with a high CO content at elevated pressures of 0.5 and 1 MPa to update the detailed chemical kinetic mechanism for hydrogen and H_2/CO (syngas) mixtures. Krejci et al. [16] measured the laminar speed of H_2/CO/air and H_2/CO/O_2/He mixtures to demonstrate the effect of carbon monoxide on H_2–O_2 chemical kinetics [15] at standard temperature and pressures up to 1 MPa. In all these studies, the experiments were conducted for mixtures at room temperature. Only Natarajan et al. [17,18], Krejci et al. [19], and Singh et al. [20] measured laminar flame speed of H_2/CO mixtures with various H_2–CO ratios at elevated initial temperature. However, the Markstein lengths of syngas at elevated initial temperature were not be given by Natarajan et al. [17,18] and Singh et al. [20]. Although Krejci et al. [19] obtained the Markstein lengths of syngas at elevated initial temperature, they focused on the effect of fuel mixture (H_2:CO ratio) and moisture content on the Markstein lengths other than the effect of elevated initial temperature on them. Recent works published on the laminar flame speed of syngas mixtures were reviewed by Lee et al. [21]. Since the syngas combustion occurs at elevated pressures and temperatures in practical combustors, fundamental research should be conducted to understand the syngas combustion characteristics at these conditions.

The objectives of the present work are to measure the laminar flame speed and Markstein length and to examine the effects of pressure and initial temperature on the flame properties of typical syngas mixtures. Unlike previous studies, the typical syngas (see Table 1, according to which the composition of the typical syngas is H_2:CO:CO_2:N_2 = 31:37.2:12:12.2) is studied using a constant pressure spherical flame technique (see [22,23] and references therein), because there is a lack of fundamental data on the laminar combustion characteristics of actual syngas fuel which is composed of H_2, CO, N_2 and CO_2. Furthermore, in order to ascertain the accuracy of the different kinetic models at conditions that are more relevant to gas-turbine combustor, the experimental data of the laminar flame speed are compared to these from numerical simulations. Besides, the experimental data of the Markstein length are used to examine the prediction from theoretical model proposed in the literature.

2. Experimental and computational methods

The major components of the facility used for experiments include a high-pressure combustion chamber, four ceramic heaters, a high voltage spark generator, and a Schlieren optical system. The schematic of the experimental facility is shown in Fig. S1 in the Supplementary Material. A pressure-release type high pressure combustion chamber, capable of withstanding pressure up to 4 MPa, was designed and fabricated. The chamber is 305 mm in length and consists of two concentric cylindrical vessels of inner diameter of 100 mm and 300 mm, respectively. One pair of optical quartz windows with diameter of 100 mm was fitted on both ends of the inner chamber. On the cylindrical surface of the inner chamber, twelve holes were made for the purpose of pressure release. These holes are sealed using high temperature O-rings under the compression of the iron plates. The pressure difference between outer and inner chambers (above 0.05 MPa) can compress the iron plates and provide completely vacuum sealing. In experiment, nitrogen is first filled into the outer chamber, and then combustible mixtures are filled into the inner vessel. The pressure of outer chamber is 0.05 MPa higher than that in the inner chamber. After ignition and flame propagation, the pressure in the inner chamber will increase till it is high enough to cause gas leakage or iron plate opening. The idea of using dual chamber is similar to that in Refs. [24,25].

Spherical flame propagation was initialized by the electrical spark at the center of vessel through two tungsten electrodes with diameters of 0.4 mm. The spark energy was adjusted to be sufficiently close to the minimum ignition energy in order to minimize the effects of ignition and unsteady transition on flame propagation [26,27]. Four ceramic heaters located in outer chamber were used to heat the combustible mixtures in the inner chamber through heat transferred from the inert gas, which is heated by the heaters firstly. The inner chamber can be heated to a maximum temperature of 500 K. The temperature of inner and outer chamber was measured by two type *K*-thermocouples (213–1023 K). The pressure at the inner and outer chambers during the gas-filling process was monitored by two absolute pressure transmitters. A compressor was used for purging the chamber before and after combustion.

The propagating spherical flame was imaged using Schlieren photography with a 300-W iodine–tungsten lamp. Light from the lamp is focused on a 100 μm pinhole and collimated by a plane-spherical lens. The collimated light passes through the inner chamber and is focused on a horizontally installed knifed edge. A high-speed digital video camera (photron SA4) with shutter speed of 10 μs and frame rate of 8000 fps was used to record the propagating spherical flame images.

The required gases (purity level: H_2-99.999%, CO-99.99%, O_2-99.999%, N_2-99.999%) were filled into inner chamber to the corresponding partial pressures using the absolute pressure gauge to prepare the required mixture. After filling, the chamber was left undisturbed for 15 min to ensure complete mixing and attainment of a quiescent condition. All the experiments were repeated at least three times.

In order to estimate the uncertainty associated with the determination of unstretched laminar flame speed, an uncertainty analysis was carried out following the procedure of Aung et al. [28]. The uncertainty of the unstretched laminar flame speed mainly comes from two sources: the uncertainty in the determination of radius, and that in the linear extrapolation of the stretched propagation velocity to zeros stretch. The overall uncertainty of unstretched laminar flame speed was estimated to be within 5%.

The laminar flame speed of the typical syngas at different equivalence ratios, pressures, and temperatures were calculated using the CHEMKIN-PREMIX code [29]. Two different detailed chemical mechanisms for syngas were used: one is the Davis-mechanism [30] consisting of 14 species and 38 elementary reactions, and the other is Sun-mechanism [11] with 16 species and 48 elementary reactions. The number of grid points was kept to be above 200 so that the flame structure was well resolved and the calculated laminar flame speed was nearly grid-independent.

Table 1
Summary of compositions (in volume fraction (%)).

Constituent	Min	Max	Avg
H_2	8.6	61.9	31
CO	22.3	55.4	37.2
CO_2	1.6	30	12
N_2	0.2	49.3	12.2
H_2/CO ratio	0.33	2.36	0.86

3. Laminar flame speed and Markstein length determination

After imaging the spherical flame, the flame front was determined by an edge detection code and then converted to flame radius. The raw data of flame radius were smoothed to avoid the local disturbances. When the pressure rise is negligible, the burned gas is motionless. Therefore, the stretched flame speed with respect to burned mixture, S_b, and the stretch rate, K, are given by the following two expressions:

$$S_b = dR_f/dt \tag{1}$$

$$K = 2S_b/R_f \tag{2}$$

where R_f is the flame radius. The unstretched laminar flame speed, S_b^0, and Markstein length, L_b, can be extracted according to the following linear relationship between stretched flame speed and stretch rate [31,32]

$$S_b = S_b^0 - L_b K \tag{3}$$

This methodology assumes that the spherical flame is infinitesimally thin, weakly stretched, quasi-steady flame in a zero-gravity, unconfined environment [33]. The radius data range of $0.01 < R_f < 0.02$ m was used to determinate the unstretched laminar flame speed and Markstein length. This range corresponds to flames of smooth surface with large ratios of radius to thickness, thus ensures the validity of the linear approximation of Eq. (3) [23]. The laminar flame speed with respect to unburned mixture, S_u^0, is determined through $S_u^0 = \sigma S_b^0$, where σ is the density ratio between the burned and unburned mixtures. In this study, the laminar flame speed is always above 0.2 m/s. Therefore, the effects of buoyancy [34] and radiation [35] on spherical flame propagation are negligible.

According to asymptotic analysis, Markstein lengths, which show how combustible mixtures are sensitive to flame stretch, can be predicted by an explicit expression [36,41,42] in terms of the fundamental flame physico-chemical parameters:

$$L_b = \left[\frac{1}{Le_{eff}} - \left(\frac{Ze}{2}\right)\left(\frac{1}{Le_{eff}} - 1\right)\right]\sigma\delta \tag{4}$$

with Le_{eff} being the effective Lewis number of the mixture, Ze the Zel'dovich number and δ the flame thickness. Eq. (4) indicates that the Markstein length depends strongly on the effective Lewis number. The effective Lewis number is defined as the ratio of the thermal diffusivity (D_T) to the mass diffusivity of the deficient reactant (D_i). Therefore, for fuel–lean mixtures the Markstein length depends on the Lewis number of the fuel and for fuel–rich mixtures it depends on the Lewis number of the oxygen. Near stoichiometry, an alternate overall effective Lewis number should be used to consider weighted average effects of the "two" reactants (fuel/oxidizer) [36]:

$$Le_{All} = 1 + \frac{(Le_{Ex} - 1) + (Le_{Def} - 1)A}{1 + A} \tag{5}$$

with $A = 1 + Ze(1/\phi - 1)$, where ϕ is the mixture equivalence ratio. The subscripts Ex and Def in Eq. (5) denote the excess and deficient reactants, respectively. As noted, syngas is composed of two fuel components, i.e. H_2 and CO. Three fuel effective Lewis number formulations for bi-component fuels were summarized by Bouvet et al. [36]. They are weighted averages of the Lewis numbers of the two fuels based on heat release, volume, and diffusion, denoted by Le_H, Le_V and Le_D respectively [36]. Since the heat of combustion per unit mass of hydrogen is nearly 12 times that of carbon monoxide, Le_H is nearly the same as Le_V. Therefore, only Le_V and Le_D were used to calculate the effective Lewis numbers in present study. According to different equivalence ratio, the effective Lewis numbers can be calculated by the following equation:

$$Le_{eff} = \begin{cases} Le_V \text{ or } Le_D & \phi \leqslant 0.8 \\ Le_{All} & 0.8 < \phi < 2.0 \\ Le_{O_2} & \phi \geqslant 2.0 \end{cases} \tag{6}$$

4. Results and discussion

4.1. Flame morphology and system validation

The Schlieren images of the spherical flame front at different pressures and initial temperatures were presented in Fig. S2 in the Supplementary Material. Smooth flame fronts were observed throughout the propagation process at normal pressure and temperature. When the initial temperature reached 460 K, large wrinkles appeared on the flame surface at 1 ms due to the disturbance of electrode. However, the large wrinkles did not further crack into small cells as the flame expanded outwardly. At $P = 0.5$ MPa and $T_u = 298$ K, the flame front of syngas/air was strongly affected by the hydrodynamic instability. This is because the flame becomes thinner at higher pressure and thus it is more easily affected by the hydrodynamic instability. The images of the third row in Fig. S2 indicated that large wrinkles appeared on the flame surface at 1 ms and then these large cells cracked into smaller ones as the flame propagates outwardly. At 4.75 ms, small cells uniformly distributed over the whole flame surface and the flame speed increased due to the increase of flame surface area. When the nitrogen was replaced by helium, a smooth surface was observed throughout the propagating process. This is due to the fact that helium addition can increase the heat conductivity and Lewis number, which helps to prevent the diffusive-thermal instability and retard the hydrodynamic instability.

In order to validate the present measurement system, we first conducted experiments for H_2/CO (50%:50% in volume) at normal and elevated temperatures. The initial pressure was fixed at $P = 0.1$ MPa. The comparisons of the present experimental results and published laminar flame speeds and Markstein lengths were provided in the Supplementary Material. Moreover, a comparison between the laminar flame speeds predicted by Davis mechanism and Sun mechanism against the present measurements is shown in Figs. S3 and S4 of the Supplementary Material. It demonstrated that the present experimental results at normal and elevated temperatures were in good agreement with those predicted by chemical mechanisms and those measured by other groups. And the Markstein lengths measured in this study were in good agreement with those of Hassan et al. [37] and Bouvet et al. [38].

4.2. Results at normal pressure and temperature

In this and the next sub-sections, all the results were for typical syngas with composition of H_2:CO:CO_2:N_2 = 31:37.2:12:12.2. To examine the effect of effective Lewis number and flame temperature on laminar flame speed of typical syngas, different oxygen–inert mixtures were used as the oxidizer. The oxygen-to-inert (He, Ar and N_2) volume ratio were fixed at 1:6, 1:3.76 and 1:3.76, for He, Ar and N_2, respectively. Helium was used to increase the effective Lewis number since its thermal conductivity is much higher than that of nitrogen while its specific heat capacity is much lower. The effective Lewis number of syngas/O_2/3.76N_2, syngas/O_2/6He, and syngas/O_2/3.76Ar are shown in Fig. 1. On the lean side, as pointed by Bouvet et al. [36], the effective Lewis numbers derived by volume-based weighted average Le_V (denoted by the solid line in Fig. 1) are obviously different from those derived by diffusion-based weighted average Le_D (denoted by the dashed line in

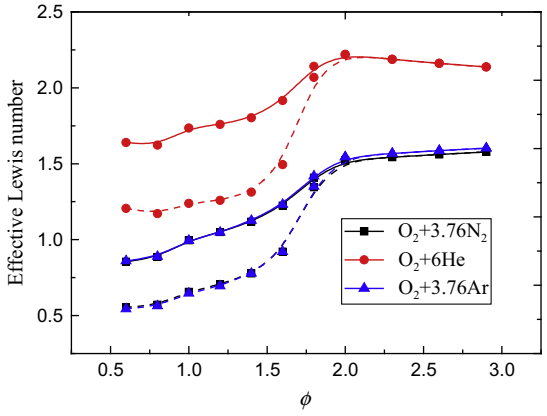

Fig. 1. Change of the effective Lewis number with the equivalence ratio. (Solid line, with Le_V; dashed line, with Le_D).

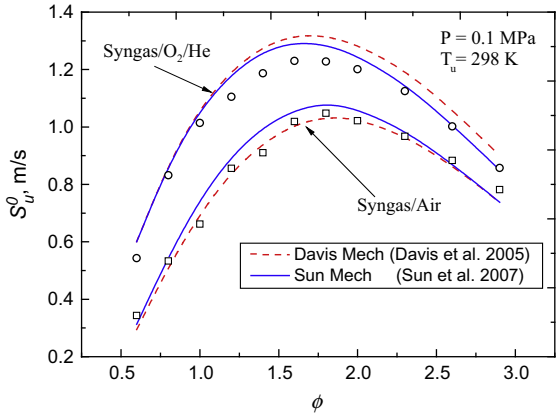

Fig. 3. Laminar flame speeds of syngas/air and syngas/O_2/He mixtures at atmospheric pressure and room temperature.

Fig. 1). For example, at $\phi = 0.6$, $Le_V = 0.855$ as $Le_D = 0.554$ for the mixture of syngas/O_2/3.76N_2. On the rich side, the solid line and the dashed line overlap, is equal to the Lewis numbers of oxygen. As shown in Fig. 1, the effective Lewis number of syngas/O_2/6He is much larger than that of syngas/O_2/3.76N_2, either Le_V or Le_D. In order to maintain the same adiabatic flame temperature, the volumetric ratio between oxygen and helium was 6.0. The results in Fig. 2 demonstrated that syngas/O_2/6He and syngas/O_2/3.76N_2 have nearly the same adiabatic flame temperature for each equivalence ratio. Argon was used to increase the adiabatic flame temperature since its specific heat capacity is much smaller than that of N_2. When the nitrogen was replaced by the same amount of argon, the adiabatic flame temperature was increased by 100–300 K, as indicated in Fig. 2. Since the thermal diffusivity was nearly unchanged when the nitrogen was replaced by the same amount of argon, Fig. 1 shows that the effective Lewis number of syngas/O_2/3.76Ar is very close to that of syngas/O_2/3.76N_2. Therefore, different oxidizers can be used to isolate and assess the effects of effective Lewis number and flame temperature. Similar strategy was used in our previous study on the ignition of hydrogen/air with diluents [39,40].

Fig. 3 shows the comparison of laminar flame speed of syngas/air mixtures with that of syngas/O_2/He mixture at normal pressure and temperature. It is seen that the laminar flame speeds of syngas/air mixtures calculated with Davis and Sun mechanisms were in agreement with the experimental results. Very good agreement was observed at lean conditions and ultra rich conditions, while the mechanism predictions were slightly higher than those from experiments for equivalence ratio within the range of $1.2 < \phi < 2.0$. The laminar flame speed for the two kinds of mixtures firstly increases with the equivalence and then begins to decrease with further increasing equivalence ratio. The peak flame speed of syngas/air mixture and syngas/O_2/He mixture is 1.048 m/s at $\phi = 1.8$ and 1.23 m/s at $\phi = 1.6$, respectively. The laminar flame speed of syngas/O_2/He mixtures was significant larger than that of syngas/air. This is due to the facts that the laminar flame speed is proportional to the square root of the Lewis number and that the Lewis number of syngas/O_2/He is much higher than that of syngas/air (see Fig. 1) while the adiabatic flame temperature is nearly the same (see Fig. 2) [41]. Fig. 4 shows the comparison of laminar flame speed of syngas/air with that of syngas/O_2/Ar at normal pressure and temperature. The flame speed of syngas/O_2/Ar calculated using Davis and Sun mechanisms was in very agreement with experimental results. The peak flame speed of syngas/O_2/Ar mixtures is 1.3 m/s at $\phi = 1.8$. As shown in Fig. 4, the comparison between flame speed of syngas/O_2/Ar with high temperature and that of syngas/air with low temperature demonstrated that the effects of flame temperature on laminar flame speed of syngas were significant.

Fig. 5 shows Markstein lengths of syngas/air, syngas/O_2/Ar, and syngas/O_2/He mixtures at normal pressure and temperature as a function of equivalence ratio. The experimental results indicate that the Markstein lengths of different mixtures increase monotonically with the equivalence ratio. The prediction from theoretical model given by Eq. (4) agrees very well with experimental results

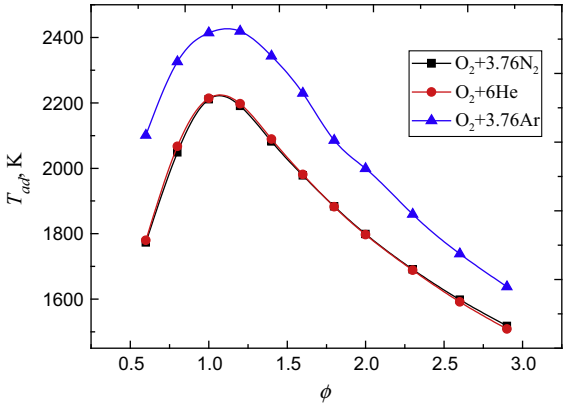

Fig. 2. Change of the adiabatic flame temperature with the equivalence ratio.

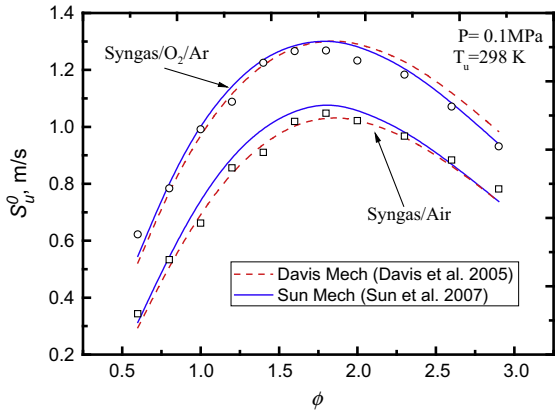

Fig. 4. Change of the Laminar flame speeds of syngas/air and syngas/O_2/Ar mixtures at atmospheric pressure and room temperature.

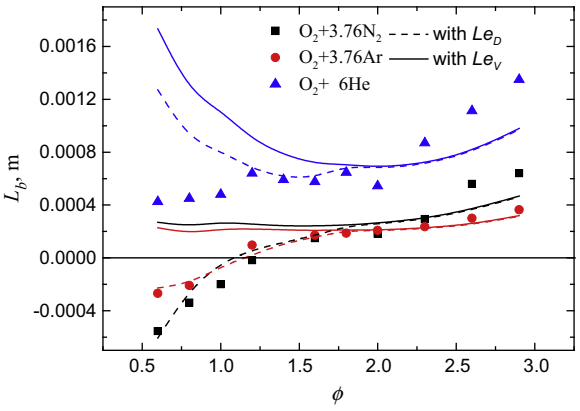

Fig. 5. Markstein length of syngas/air, syngas/O_2/Ar and syngas/O_2/He mixtures at normal pressure and temperature. The symbols stand for experimental results and the lines are prediction from Eq. (4).

for syngas/air and syngas/O_2/Ar when Le_D is used. However, for syngas/O_2/He good agreement is achieved only for fuel-rich case with $\phi > 1.2$. Moreover, Fig. 5 demonstrates that more accurate Markstein length can be predicted by using Le_D than using Le_V. The same conclusion was drawn for syngas in [36]. It is noted that for lean hydrogen/hydrocarbon/air mixtures instead of syngas/air mixtures, Bouvet et al. [36] showed that Le_V should be used to evaluate the Markstein length. The Markstein length of syngas/air mixture was close to that of syngas/O_2/Ar mixture. This is because the effective Lewis number of these two mixtures is nearly the same for each equivalence ratio as shown in Fig. 1. However, Fig. 5 showed that the Markstein length of syngas/O_2/He mixture was always positive and it was much higher than that of syngas/air mixture. As a result, replacement of nitrogen by helium can prevent the diffusive-thermal instability and retard the hydrogen instability.

4.3. Results at elevated pressures and temperatures

Fig. 6 shows laminar flame speeds of syngas/O_2/He mixture at different pressures. It is seen that the laminar flame speed predicted by Davis and Sun mechanisms was in agreement with the experimental results. The laminar flame speed at different pressures increases with equivalence and begins to decline with further increasing equivalence ratio. The peak value of the flame speed was 0.867 m/s at $P = 1$ MPa and 1.059 m/s at $P = 0.5$ MPa, respectively. Moreover, Fig. 6 shows that the laminar flame speed decreases with the increase of the pressure. The dependence of the laminar flame speed on pressure can be readily assessed from the following formula, $S_u^0 = f^0/\rho_u$, where f^0 is the laminar mass flux, ρ_u is the density of unburned mixture. The effect of pressure on laminar burning flux can be determined through the overall reaction order n, as $f^0 \sim P^{n/2}$, then, the density of unburned mixture varies proportionally with the pressure, as $\rho_u \sim P$, so $S_u^0 \sim P^{(n/2-1)}$. In the pressure range investigated, the inhibiting reaction $H + O_2 + M \rightarrow HO_2 + M$ is enhanced as pressure increases, which reduces the H atom concentration and competes with the chain-branching reaction producing free radicals O and OH:$H + O_2 \rightarrow OH + O$ [26]. A retarding effect is therefore imposed on the overall progress of the reaction with increasing pressure, causes the decrease in n. At the same time, the unburned mixture also becomes denser for the flame to heat up and pass through as pressure increases. Consequently, the increased density effect and the retarding chemical effect reduce the laminar flame speed [41].

Fig. 7 shows laminar flame speeds of syngas/air mixture at three different initial temperatures. As expected, the laminar flame speed increases with the initial temperature. With the increase in the initial temperature, the adiabatic flame temperature increases and hence the reaction rates become larger [41]. As shown in Fig. 7, with the increase of initial temperature, the discrepancy between the measured and calculated flame speed increases, especially at the rich conditions. For $T_u = 380$ K and $\phi \geqslant 1.8$, the laminar flame speed was greatly under predicted by both mechanisms. Therefore, the present experimental results indicated that the syngas mechanisms of Davis and Sun were not suitable for rich syngas/air at elevated temperatures and these mechanisms should be improved.

The Markstein length characterizes the variation in the local flame speed due to the influence of external stretching. Fig. 8 shows Markstein lengths of syngas/O_2/He at different pressures. It is seen that the Markstein length increases with the equivalence ratio, indicating that the spherical flame propagation speed is more sensitive to the stretch rate and more stable for rich syngas/O_2/He mixtures than lean mixtures. Furthermore, the Markstein length is shown to decrease with the pressure. This is due to the fact that the flame thickness becomes smaller at higher pressures. As mentioned earlier, neither the theoretical model of Markstein length combined with Le_V nor with Le_D can reproduce the increasing trend with the equivalence ratio for syngas/O_2/He. They can predict the decreasing trend with the pressure, but overestimate the Markstein lengths at elevated pressure. Fig. 9 plots the Markstein lengths of syngas/air at different initial temperatures as a function of equivalence ratio. It is seen that the Markstein lengths at elevated initial temperatures also increase

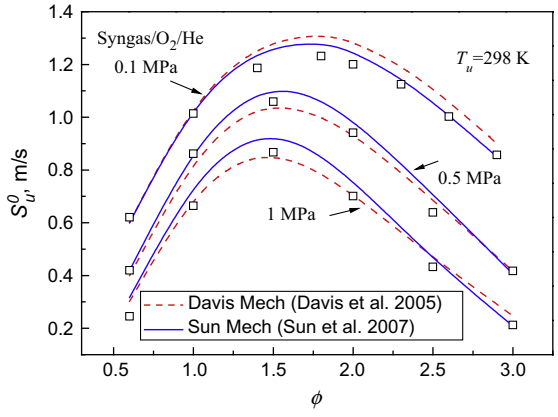

Fig. 6. Laminar flame speeds of syngas/O_2/He mixtures at normal and elevated pressures.

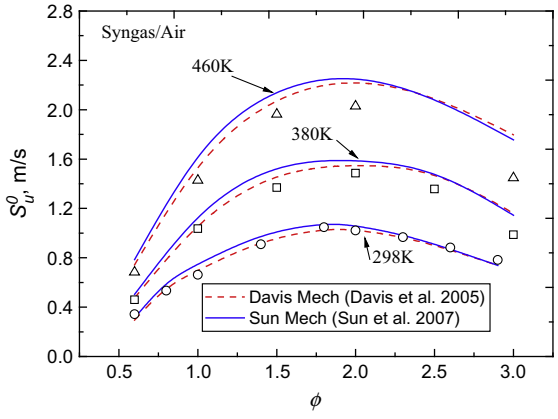

Fig. 7. Laminar flame speeds of syngas/air mixtures at normal and elevated temperatures.

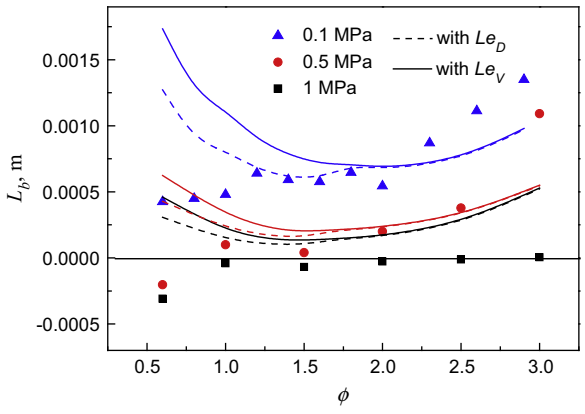

Fig. 8. Markstein length of syngas/O_2/He mixtures at different pressures. The initial temperature is fixed to be T_u = 298 K. The symbols stand for experimental results and the lines are prediction from Eq. (4).

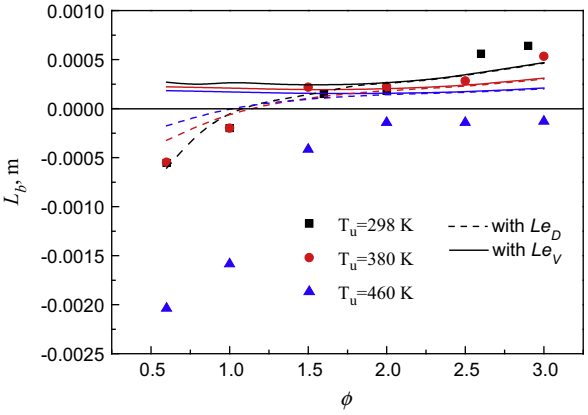

Fig. 9. Markstein length of syngas/air mixtures at different initial temperatures. The pressure is fixed to be P = 0.1 MPa. The symbols stand for experimental results and the lines are prediction from Eq. (4).

with the equivalence ratio. The Markstein lengths at T_u = 300 K were close to those at T_u = 380 K, especially on the lean side. With the increase of the initial temperature to T_u = 460 K, the Markstein length is reduced. As the pressure case, the theoretical models of Markstein length overestimate the Markstein lengths at high initial temperature either.

In summary, the Markstein length decreases from positive values to negative values with the increase of pressure and initial temperature, indicating the distinct stretch effects on flame propagation at elevated pressure and initial temperature from those at normal conditions.

5. Conclusion

Experiments on typical syngas/O_2/diluent flames were conducted at normal and elevated pressures and temperatures using a high-pressure combustion chamber. The laminar flame speed and Markstein length were measured and the effects of Lewis number, flame temperature, pressure and initial temperature were examined. The main conclusions are:

1. Different oxidizers can be used to isolate and assess separately the effects of Lewis number and flame temperature. When the adiabatic flame temperature remained unchanged (syngas/O_2/6He vs. syngas/O_2/3.76N_2), the Lewis number was shown to have significant influence on laminar flame speed. When the Lewis number was fixed (syngas/O_2/3.76Ar vs. syngas/O_2/3.76N_2), increase of the adiabatic flame temperature resulted in the increase of the laminar flame speed.
2. The laminar flame speeds of syngas/O_2/diluent mixtures at different equivalence ratios were measured at normal and elevated pressures and temperatures. These data were used to assess the performance of different chemical mechanisms for syngas. At room temperature, the laminar flame speeds measured in this study were shown to be accurately predicted by syngas mechanisms available in the literature. However, at elevated temperature, the laminar flame speeds measured in this study were greatly under predicted by the syngas mechanisms of Davis et al. [30] and Sun et al. [11]. Therefore, the present experimental results indicated that the syngas mechanisms of Davis et al. [30] and Sun et al. [11] were not suitable for rich syngas/air at elevated temperatures and should be improved.
3. The Markstein lengths of syngas/O_2/diluent mixtures at different equivalence ratios were also measured at normal and elevated pressures and temperatures. It was found that the Markstein length decreased with the increase of pressure and initial temperature. Moreover, the Markstein length was less sensitive to the change of initial temperature than that of pressure.
4. The prediction from theoretical model for Markstein length was found to agree well with experimental data only at normal temperature and pressure. Obvious difference between model prediction and experimental results was observed for fuel–lean mixtures at elevated temperature/pressure. Moreover, it was found that for syngas, the diffusion-based Lewis number rather than the volume or heat release-based Lewis number should be used to evaluate the Markstein length from the theoretical model of syngas.

Acknowledgments

This work is supported by National Natural Science Foundation of China (NSFC) under Grant Nos. 51406200, 50976115 and 51322602. Financial supports from the MOST of PR China under Grant No. 2011AA050606 and the National Basic Research Program of China (No. 2014CB239600) are gratefully acknowledged.

Appendix A. Supplementary material

Supplementary data associated with this article can be found, in the online version, at http://dx.doi.org/10.1016/j.fuel.2014.08.004.

References

[1] <http://www.netl.doe.gov/technologies/coalpower/turbines/refshelf/handbook/TableofContents.html> (accessed 09.06.2011).
[2] Ge B, Zang S, Guo P, Tian Y. Experimental investigation of double-swirled non-premixed syngas flames by planar laser-induced fluorescence. Energy Fuels 2012;26:1585–91.
[3] Zhou Z, Tao ZQ, Lin BY, Kong WJ. Numerical investigation on effects of high initial temperatures and pressures on flame behavior of CO/H_2/air mixtures near the dilution limit. Int J Hydrogen Energy 2013;38:274–81.
[4] Hu EJ, Fu J, Jiang X, Huang ZH, Zhang Y. Experimental and numerical study on the effect of composition on laminar burning velocities of H_2/CO/N_2/CO_2/air mixtures. Int J Hydrogen Energy 2012;37:18509–19.
[5] Vu TM, Park J, Kown OB, Bae DS, Yun JH, Keel SI. Effects of diluents on cellular instabilities in outwardly propagating spherical syngas–air premixed flames. Int J Hydrogen Energy 2010;35:3868–80.
[6] Ding N, Arora R, Norconk M, Lee SY. Numerical investigation of diluent influence on flame extinction limits and emission characteristic of lean-premixed H_2–CO (syngas) flames. Int J Hydrogen Energy 2011;36:3222–31.
[7] Burbano HJ, Pareja J, Amell AA. Laminar burning velocities and flame stability analysis of H_2/CO/air mixtures with dilution of N_2 and CO_2. Int J Hydrogen Energy 2011;36:3232–42.
[8] Peters N. Turbulent combustion. New York: Cambridge University Press; 2000.

[9] McLean IC, Smith DB, Taylor SC. The use of carbon monoxide/hydrogen burning velocities to examine the rate of the CO + OH reaction. Symp (Int) Combust 1994;25:749–57.
[10] Brown MJ, McLean IC, Smith DB, Taylor SC. Markstein lengths of CO/H_2/air flames, using expanding spherical flames. Symp (Int) Combust 1996;26:875–81.
[11] Sun HY, Yang SI, Jomaas G, Law CK. High pressure laminar flame speeds and kinetic modeling of carbon monoxide/hydrogen combustion. Proc Combust Inst 2007;31:439–46.
[12] Burke MP, Chaos M, Dryer FL, Ju Y. Negative pressure dependence of mass burning rates of H_2/CO/O_2/diluent flames at low flame temperatures. Combust Flame 2010;157:618–31.
[13] Prathap C, Ray A, Ravi MR. Investigation of nitrogen dilution effects on the laminar burning velocity and flame stability of syngas fuel at atmospheric condition. Combust Flame 2008;155:145–60.
[14] Prathap C, Ray A, Ravi MR. Effects of dilution with carbon dioxide on the laminar burning velocity and flame stability of H_2–CO mixtures at atmospheric condition. Combust Flame 2012;159:482–92.
[15] Kéromnès A, Metcalfe WK, Heufer KA, Donohoe N, Das AK, Sung CJ, et al. An experimental and detailed chemical kinetic modeling study of hydrogen and syngas mixture oxidation at elevated pressures. Combust Flame 2013;160:995–1011.
[16] Krejci MC, Mathieu O, Vissotski AJ, Ravi S, Sikes TG, Petersen E. Laminar flame speed and ignition delay time data for the kinetic modeling of hydrogen and syngas fuel blends. J Eng Gas Turbines Power 2013;135:021503–21509.
[17] Natarajan J, Lieuwen T, Seitzman J. Laminar flame speeds of H_2/CO mixtures: effect of CO_2 dilution, preheat temperature, and pressure. Combust Flame 2007;151:104–19.
[18] Natarajan J, Kochar Y, Lieuwen T, Seitzman J. Pressure and preheat dependence of laminar flame speeds of H_2/CO/CO_2/O_2/He mixtures. Proc Combust Inst 2009;32:1261–8.
[19] Krejci M, Vissotski A, Ravi S, Metcalfe W, Keromnes A, Curran H, et al. Laminar flame speed measurements of moist syngas fuel blends at elevated pressures and temperatures. In: Spr tech meeting (CSSCI); 2012. p. 1–8.
[20] Singh D, Nishiie T, Tanvir S, Qiao L. An experimental and kinetic study of syngas/air combustion at elevated temperatures and the effect of water addition. Fuel 2012;94:448–56.
[21] Lee HC, Jiang LY, Mohamad AA. A review on the laminar flame speed and ignition delay time of syngas mixtures. Int J Hydrogen Energy 2006;31:2310–28.
[22] Chen Z, Burke MP, Ju Y. Effects of compression and stretch on the determination of laminar flame speeds using propagating spherical flames. Combust Theory Model 2009;13:343–64.
[23] Chen Z. On the extraction of laminar flame speed and Markstein length from outwardly propagating spherical flames. Combust Flame 2011;58:291–300.
[24] Tse SD, Zhu DL, Law CK. Morphology and burning rates of expanding spherical flames in H_2/O_2/inert mixtures up to 60 atmospheres. Proc Combust Inst 2000;28:1793–800.
[25] Qin X, Ju Y. Measurements of burning velocities of dimethyl ether and air premixed flames at elevated pressures. Proc Combust Inst 2005;30:233–40.
[26] Bradley D, Gaskell PH, Gu XJ. Burning velocities, Markstein lengths, and flame quenching for spherical methane–air flames: a computational study. Combust Flame 1996;104:176–98.
[27] Chen Z, Burke MP, Ju Y. Effects of Lewis number and ignition energy on the determination of laminar flame speed using propagating spherical flames. Proc Combust Inst 2009;32:1253–60.
[28] Aung KT, Hassan MI, Faeth GM. Flame stretch interactions of laminar premixed hydrogen/air flames at normal temperature and pressure. Combust Flame 1997;109:1–24.
[29] Kee RJ, Grcar JF, Smooke MD, Miller JA. PREMIX: a fortran program for modelling steady laminar one-dimensional premixed flames. Sandia National Laboratories Report; 1985. (SAND 85-8240B).
[30] Davis SG, Joshi AV, Wang H, Egolfopoulos F. An optimized kinetic model of H_2/CO combustion. Proc Combust Inst 2005;30:1283–92.
[31] Clavin P. Dynamic behavior of premixed flame fronts in laminar and turbulent flows. Prog Energy Combust Sci 1985;11:1–59.
[32] Law CK, Sung CJ. Structure, aerodynamics, and geometry of premixed flamelets. Prog Energy Combust Sci 2000;26:459–505.
[33] Burke MP, Chen Z, Ju Y, Dryer FL. Effect of cylindrical confinement on the determination of laminar flame speeds using outwardly propagating flames. Combust Flame 2009;156:771–9.
[34] Qiao L, Gu YX, Dam WJA, Oran ES, Feath GM. Near-limit laminar burning velocities of microgravity premixed hydrogen flames with chemically-passive fire suppressants. Proc Combust Inst 2007;31:2701–9.
[35] Chen Z. Effects of radiation and compression on propagating spherical flames of methane/air mixtures near the lean flammability limit. Combust Flame 2010;157:2267–76.
[36] Bouvet N, Halter F, Chauveau C, Yoon Y. On the effective Lewis number formulations for lean hydrogen/hydrocarbon/air mixtures. Int J Hydrogen Energy 2013;38:5949–60.
[37] Hassan MI, Aung KT, Faeth GM. Properties of laminar premixed CO/H_2/air flames at various pressures. J Propul Power 1997;13:239–45.
[38] Bouvet N, Chauveau C, Gokalp I, Halter F. Experimental studies of the fundamental flame speeds of syngas (H_2/CO)/air mixtures. Proc Combust Inst 2011;33:913–20.
[39] Zhang W, Chen Z, Kong W. Effects of diluents on the ignition of premixed H_2/air mixtures. Combust Flame 2012;159:151–60.
[40] Chen Z, Burke MP, Ju Y. On the critical flame radius and minimum ignition energy for spherical flame initiation. Proc Combust Inst 2011;33:1219–26.
[41] Law CK. Combustion physics. New York: Cambridge University Press; 2006.
[42] Chen Z, Ju Y. Theoretical analysis of the evolution from ignition kernel to flame ball and planar flame. Combust Theory Model 2007;11:427–53.